Lawrence Berkeley National Laboratory

Recent Work

Title
Monte Carlo Simulations of a Hydrophobic Weak Polyelectrolyte. Charge Distribution as a Function of Conformation

Permalink
https://escholarship.org/uc/item/4km4n1hw

Journal
Journal of Chemical Physics, 99(5)

Authors
Abascal, J.L.F.
Sassi, A.P.
Blanch, H.W.
et al.

Publication Date
1993-03-01

Lawrence Berkeley Laboratory

UNIVERSITY OF CALIFORNIA

CHEMICAL SCIENCES DIVISION

Monte Carlo Simulations of a Hydrophobic Weak Polyelectrolyte. Charge Distribution as a Function of Conformation

J.L.F. Abascal, A.P. Sassi, H.W. Blanch, and J.M. Prausnitz

March 1993

DISCLAIMER

DISCLAIMER

Monte Carlo Simulations of a

Hydrophobic Weak Polyelectrolyte.

Charge Distribution as a Function of Conformation

J. L. F. Abascal*, Alexander P. Sassi,

Harvey W. Blanch and John M. Prausnitz**

Department of Chemical Engineering

University of California, Berkeley

and

Chemical Sciences Division

Lawrence Berkeley Laboratory

Berkeley, CA 94720

*Present address: Departamento de Química Física, Facultad Químicas, Ciudad Universitaria, 28040 Madrid, Spain
**To whom correspondence may be addressed.

MONTE CARLO SIMULATIONS OF A HYDROPHOBIC WEAK POLYELECTROLYTE.
CHARGE DISTRIBUTION AS A FUNCTION OF CONFORMATION

J. L. F. Abascal*, Alexander P. Sassi,

Harvey W. Blanch and John Prausnitz**

Chemical Engineering Department, University of California

and

Chemical Sciences Division, Lawrence Berkeley Laboratory

Berkeley, CA 94720

ABSTRACT

Monte Carlo simulations were performed to obtain the distribution of charged segments around the center of mass in an isolated, lattice-model, weak polyelectrolyte with attractive segment-segment (hydrophobic) interactions. Analysis of the configurations of grand-canonical ensemble Monte Carlo simulations gives the effect of polymer hydrophobicity, solution ionic strength, pH and fraction of ionizable segments. It is shown that the charge distribution (relative to the mean ionization for a given state) depends essentially on chain conformation (stiffness). For compact coil conformations, the outermost ionizable segments are mostly charged, and segments close to the center of mass of the coil remain uncharged. However, for extended conformations, the distribution of charges is nearly uniform.

* Present address: Departamento de Química Física, Facultad Químicas, Ciudad Universitaria, 28040 Madrid, Spain

**To whom correspondence should be addressed.

I. INTRODUCTION

The conformational behavior of an individual polymer chain determines many of its solution properties. For polyelectrolytes, the electrostatic interactions give rise to a rich variety of solution properties that are important in biological systems and in technological applications.

Conformational properties of an isolated polyelectrolyte chain (mean square end-to-end distance, mean square radius of gyration, finite-chain persistence length, etc) have been studied by numerous authors (e.g. 1-19). Simplified polyelectrolyte models, while retaining the essential features of the system, allow studies of larger regions of phase space than would be possible for more sophisticated descriptions. Two such simplified models are widely used in Monte Carlo simulation: the flexible chain model and the lattice model. Carnie et al (9-11) and Valleau (15) investigated a flexible-chain model of hard spheres connected by rigid bonds of fixed length and angle. In our previous work (17-19), we have used a lattice representation. The simplicity of the lattice model has made possible incorporation of the effect of hydrophobicity and observation of the concomitant structural transition in response to chain ionization (18). Most recently, we have used the lattice model in the grand-canonical Monte-Carlo simulation to study pH-induced structural transitions in hydrophobic, weak polyelectrolytes (19). For simulations in the grand-canonical ensemble, the ionization state of each of the ionizable segments is not constant but fluctuates in response to the local charge environment. The charge density is not necessarily uniform because the charges may be unevenly distributed, depending on the local environment. The objective of this work is to report briefly the charge distribution obtained from grand-canonical simulations of a hydrophobic, weak polyelectrolyte.

II. METHODS

The model and simulation method used in this work are described in Refs. 18 and 19. We summarize here the main features of our model. The polymer is represented as a self-avoiding walk of N segments on a cubic lattice. The fraction of potentially ionizable beads, λ, is 0.325 for comparison to previous work (19). The interaction between ionized segments is described by a screened Debye-Hückel coulombic potential:

$$u_{ij} = \frac{z_i \ z_j \ e^2}{D \ r_{ij}} \ \exp(-\kappa \ r_{ij})$$

where segments i and j carrying charges $z_i e$ and $z_j e$ are separated by distance r_{ij}. The dielectric constant, D, is that of water at 25°C. The effect of free ions is included through the dependence of the inverse Debye screening length, κ, on ionic strength. We consider the polyelectrolyte at

2

infinite dilution; thus, its charge is not taken into account in the evaluation of κ. Non-bonded nearest-neighbor segments interact with a fixed potential, ε; we only consider the case $\varepsilon \leq 0$ to represent polymer hydrophobicity.

Taking the ionizable groups to be basic, new configurations in the grand canonical ensemble are accepted based on the probability

$$p_{s+1} = min\{1, exp[(-\Delta E/kT) + \Delta m_c(pK_o\text{-}pH)ln10]\}$$

where ΔE is the energy change in going from configuration s to s+1, and Δm_c is the change in the number of ionized segments from configuration s to s+1. K_0 is the intrinsic dissociation constant of the protonated segment; i.e. the value that the dissociation constant would take in the absence of interactions between the charged groups. The configurations were obtained using the Metropolis Monte Carlo method and recorded every 3000 attempted moves. Details of the simulations are given in our previous paper (19).

To characterize the charge distribution, we define the function q(r) as the quotient of the intramolecular distribution function for charged segments ($g_{intra}^{ch}(r)$) and that for all segments, irrespective of ionization state($g_{intra}(r)$):

$$q(r) = \frac{g_{intra}^{ch}(r)}{g_{intra}(r)}$$

where $g_{intra}^{ch}(r)$ is the ensemble average of the number of charged segments at distance r normalized to the number of sites at r and $g_{intra}(r)$ is the ensemble average of the number of segments at r normalized to the number of sites at r. The charge distribution q(r) therefore gives the probability that a segment at distance r from the center of mass is charged. The mean ionization of the chain, α, is then given by

$$\alpha = \frac{1}{N}\int g_{intra}^{ch}(r)r^2dr$$

where N is the number of segments in the chain.

III. RESULTS AND DISCUSSION

The complex interplay between ionization state and conformation in a hydrophobic polyelectrolyte gives rise to a rich set of titration and conformational properties. In simplified modelling of systems containing polyelectrolytes, common practice is to treat the polyelectrolyte

as a cylinder with its charge uniformly smeared on the surface (20), as a Gaussian chain of charged segments (21,22), or as a chain of globular blobs (23,24). However, the majority of the cases considered (by theory or simulation) refer to strong polyelectrolytes where each segment is charged. Thus, the charged-segment distribution is straight-forward. In our model, not every ionizable segment is necessarily ionized, and the locations of the ionized segments are not fixed during the simulation. These conditions imply that the distribution of charged segments may be sensitive to conformation.

Figures 1 and 2 present the charge distribution $q(r)$ as a function of r non-dimensionalized by the lattice length, l, for a 40-segment chain with $\lambda = 0.325$. Figure 1 shows results for pH-$pK_0 = -2.5$ and the cases $\varepsilon/kT=0$, $\kappa^{-1} = 9.62$Å (0.1M), $\varepsilon/kT=-1.0$, $\kappa^{-1}=9.62$ Å (0.1M) and $\varepsilon/kT=0$, $\kappa^{-1}=96.2$Å (0.001M), where M refers to the molarity of a 1-1 electrolyte. In Figure 2, results are shown for pH-$pK_0 = -1.0$ and the same combinations of hydrophobicity and ionic strength. The cutoff of $q(r)$ in these figures is at the distance r which includes, on average, approximately 95% of the segments. As all the curves correspond to chains with the same number of segments, the mean rigidity of the polyelectrolyte at any state is reflected in the maximum value of r displayed in the corresponding plot. The mean ionization, α, is shown as a dashed line reaching each curve.

As previously reported (19), there is a close relationship between chain conformation (chain stiffness) and α. The same holds true for the shape of the $q(r)$ curves. Despite the wide variety of conditions studied, the distribution of charges around the center of mass is determined essentially by chain stiffness. If the overall conditions lead to a highly ionized polyelectrolyte, the chain assumes an expanded conformation because of electrostatic repulsion between charged groups. In the limiting case of linear (or staircase) conformations, these repulsive interactions should produce a uniform distribution of charges along the chain. In the absence of hydrophobicity and at a pH such that most ionizable segments are protonated, a nearly uniform charge density is observed, as in the case $\varepsilon/kT=0$, $\kappa^{-1} = 9.62$Å in Fig. 1. For this case, the value of $q(r)$ is roughly equal to the maximum attainable ionization of 0.325 and falls at higher values of r/l because the outermost segments are not ionizable (19). We also note that the maximum value of r/l for a staircase conformation is $(N/6)\sqrt{3} = 10.5$ for a 40-segment chain, which is approximately the maximum value of r for the case $\varepsilon/kT=0$, $\kappa^{-1} = 9.62$Å in Fig. 1.

The opposite situation is that of compact chain conformation due to low chain ionization, hydrophobic forces and/or highly screened electrostatic interactions (high ionic strength). This situation is illustrated to varying degrees in Figure 2 by the cases $\varepsilon/kT=0$, $\kappa^{-1}=96.2$Å and $\varepsilon/kT=-1.$, $\kappa^{-1}=9.62$Å. In these cases, the charges are preferentially located near the surface of the chain whereas the inner segments are mostly uncharged. Consequently, $q(r)$ exceeds α for all but the smallest values of r.

The remaining cases studied are intermediate between the two aforementioned extremes. As the chain expands, the charge distribution, $q(r)$, tends to flatten. For $\varepsilon/kT = 0$, $\kappa^{-1}=9.62\text{Å}$ in Fig. 2, for example, the lack of attractive interactions tends to allow preferentially extended conformations with chain ionization, and thus a uniform $q(r)$. However, the moderate electrostatic screening tends to compact the chain at any given ionization. The net result of these competing effects is a moderately extended conformation. As a consequence, the initial slope of the $q(r)$ curve is shallow.

Figure 3 shows $q(r)$ for two chains differing only in the number of segments where $\varepsilon/kT= -1$, $\kappa^{-1}=9.62\text{Å}$ and $pH-pK_o = -1$. The mean ionization of the chain with 100 segments is approximately the same as that for 40 segments, but, since the 100-segment chain is larger, there is a redistribution of charges toward the surface, and the shape of $q(r)$ is flattened.

The variables of the system (λ, ε/kT, κ, pH, pK_o) in concert determine polymer ionization and conformation. However, once ionization and conformation are known, it appears possible to describe approximately the distribution of charges in a manner independent of the conditions by which the chain achieved its ionization and conformation as shown in Figure 4 where the ratio of $q(r)$ to its mean value, α, is plotted as a function of radial distance reduced with the square root of the mean square radius of gyration, $<s^2>^{0.5}$. All curves cross approximately at the point (1,1) indicating that, for any combination of system variables, the average charge at a radial distance representing the mean extension of the chain is the mean ionization. The changes in shape of the curve are gradual and can essentially be defined by the initial slope, which is related to α and s^2. We did not attempt to correlate the initial slope to α and s^2 because of the large number of systems needed for such a study.

IV. CONCLUSIONS

We have examined the radial distribution of charges for a lattice-model, hydrophobic, weak polyelectrolyte using Monte-Carlo simulation methods. If the polymer chain is highly collapsed, the charges are clustered predominantly on the surface, and the surface ionization is significantly greater than the average ionization, α. If, however, the charge density is sufficient to expand the chain into a staircase conformation, the charge density is almost constant throughout the chain.

ACKNOWLEDGMENTS

FIGURE CAPTIONS:

Figure 1. Charge distribution as a function of distance to the center of mass for pH-pK $_0$ = -2.5. Closed circles denote the case $\varepsilon/kT = 0$, $\kappa^{-1} = 9.62$Å (0.1M); Open circles denote the case $\varepsilon/kT = -1$, $\kappa^{-1} = 9.62$Å (0.1M); Triangles denote the case $\varepsilon/kT = 0$, $\kappa^{-1} = 96.2$Å (0.001M). Dashed lines show the mean ionization α for the corresponding conditions. Full lines are a guide to the eye.

Figure 2. Same as Fig. 1 but for pH-pK $_0$ = -1. Asterisks denote the case $\varepsilon/kT = 0$, $\kappa^{-1} = 9.62$Å (0.1M). Squares denote the case $\varepsilon/kT = -1$, $\kappa^{-1} = 9.62$ Å (0.1M). Triangles denote the case $\varepsilon/kT = 0$, $\kappa^{-1} = 96.2$Å (0.001M).

Figure 3. Effect of chain length on the shape of the charge distribution function for pH-pK $_0$ = -1, $\varepsilon/kT = -1$, $\kappa^{-1} = 9.62$Å. Circles are for N=40; Triangles are for N=100.

Figure 4. Charge distribution relative to mean ionization as a function of radial distance reduced with the square root of the mean square radius of gyration. The symbols are the same as those in Figs. 1 and 2.

REFERENCES

1. A. Baumgärtner, J. Physique Lett., 45, L-515 (1984).

2. C. Brender, M. Lax and S. Windwer, J. Chem. Phys., 74, 2576 (1981).

3. C. Brender, M. Lax and S. Windwer, J. Chem. Phys., 80, 886 (1984).

4. C. Brender, J. Chem. Phys., 92, 4468 (1990).

5. C. Brender, J. Chem. Phys., 93, 2736 (1990).

6. C. Brender, J. Chem. Phys., 94, 3213 (1991).

7. C. Brender and M. Danino, J. Chem. Phys., 97, 2119 (1992).

8. S.L. Carnie, G.A. Christos and T.P. Creamer, J. Chem. Phys. 89, 6484 (1988).

9. G.A. Christos and S.L. Carnie, J. Chem. Phys., 91, 439 (1989).

10. G.A. Christos and S.L. Carnie, J. Chem. Phys., 92, 7661(1990).

11. G.A. Christos, S.L. Carnie and T.P. Creamer., Macromolecules, 25, 1121 (1992).

12. P.G. Higgs and H. Orland, J. Chem. Phys., 95, 4506 (1991).

13. C.E. Reed and W.F. Reed, J. Chem. Phys., 94, 8479 (1991).

14. C.E. Reed and W.F. Reed, J. Chem. Phys., 96, 1609 (1992).

15. J.P. Valleau, Chem. Phys. 129, 163 (1989).

16. C.E. Woodward and Bo Jönsson, Chemical Physics, 155, 207 (1991).

17. H.H. Hooper, H.W. Blanch, and J.M. Prausnitz, Macromolecules, 23, 4820 (1990).

18. H.H. Hooper, S. Beltrán, A.P. Sassi, H.W. Blanch, J.M. Prausnitz, and R.A. Siegel, J. Chem. Phys., 93, 2715 (1990).

19. A.P. Sassi, S. Beltrán, H.H. Hooper, H.W. Blanch, J.M. Prausnitz, and R.A. Siegel, J. Chem. Phys., 97, 8767 (1992).

20. L. Kotin and M. Nagasawa, J. Chem. Phys., 36, 873 (1962).

21. W. Kuhn, D. Kunzle and A. Katchalsky, Helv. Chim. Acta, 31, 1994 (1948).

22. J. Hermans and J. Overbeek, Receuil Travaux Chimiques, 67, 761 (1968).

23. P.G. de Gennes, P. Pincus and R.M. Velasco, J. Physique, 37, 1461 (1976).
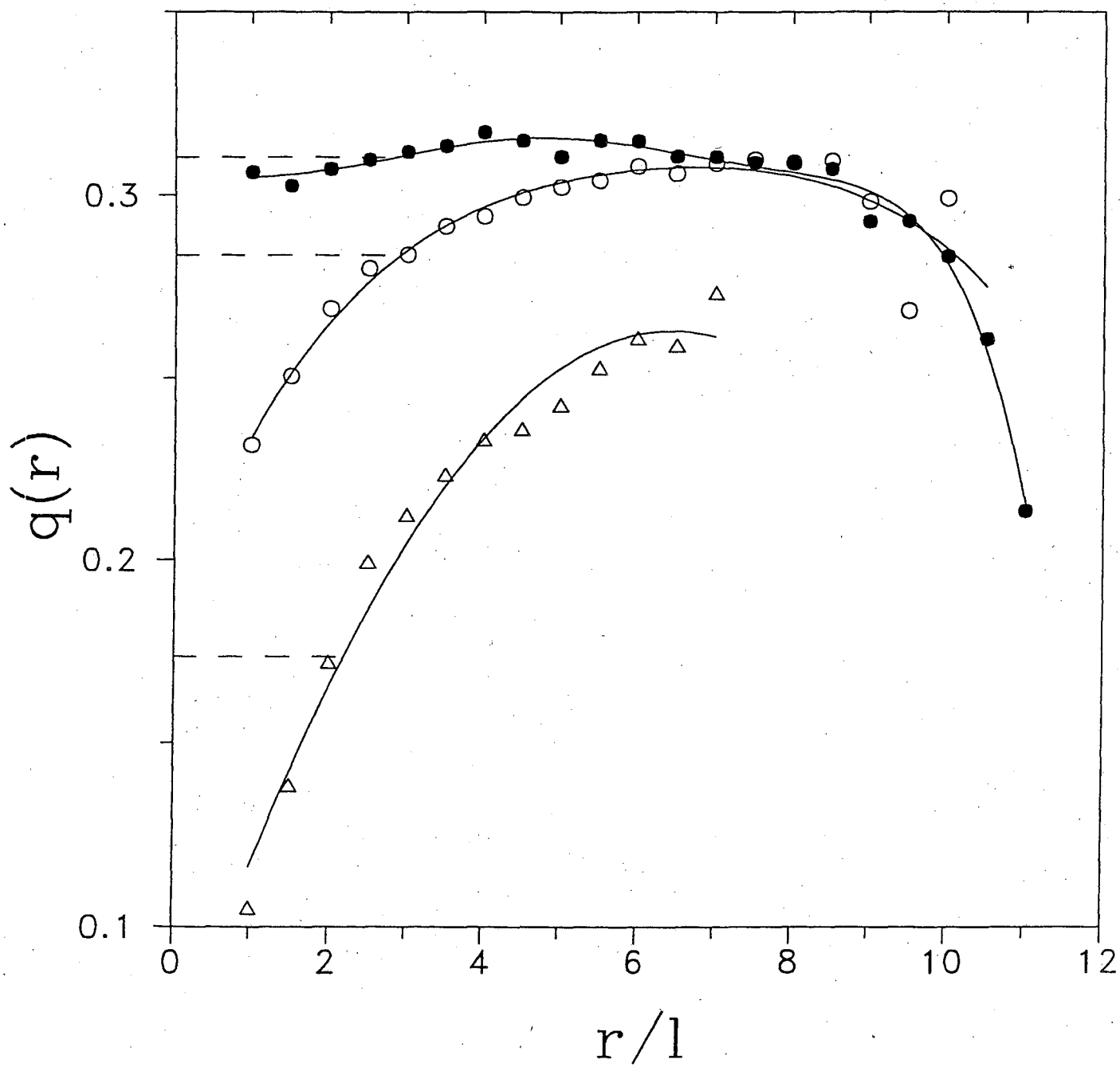
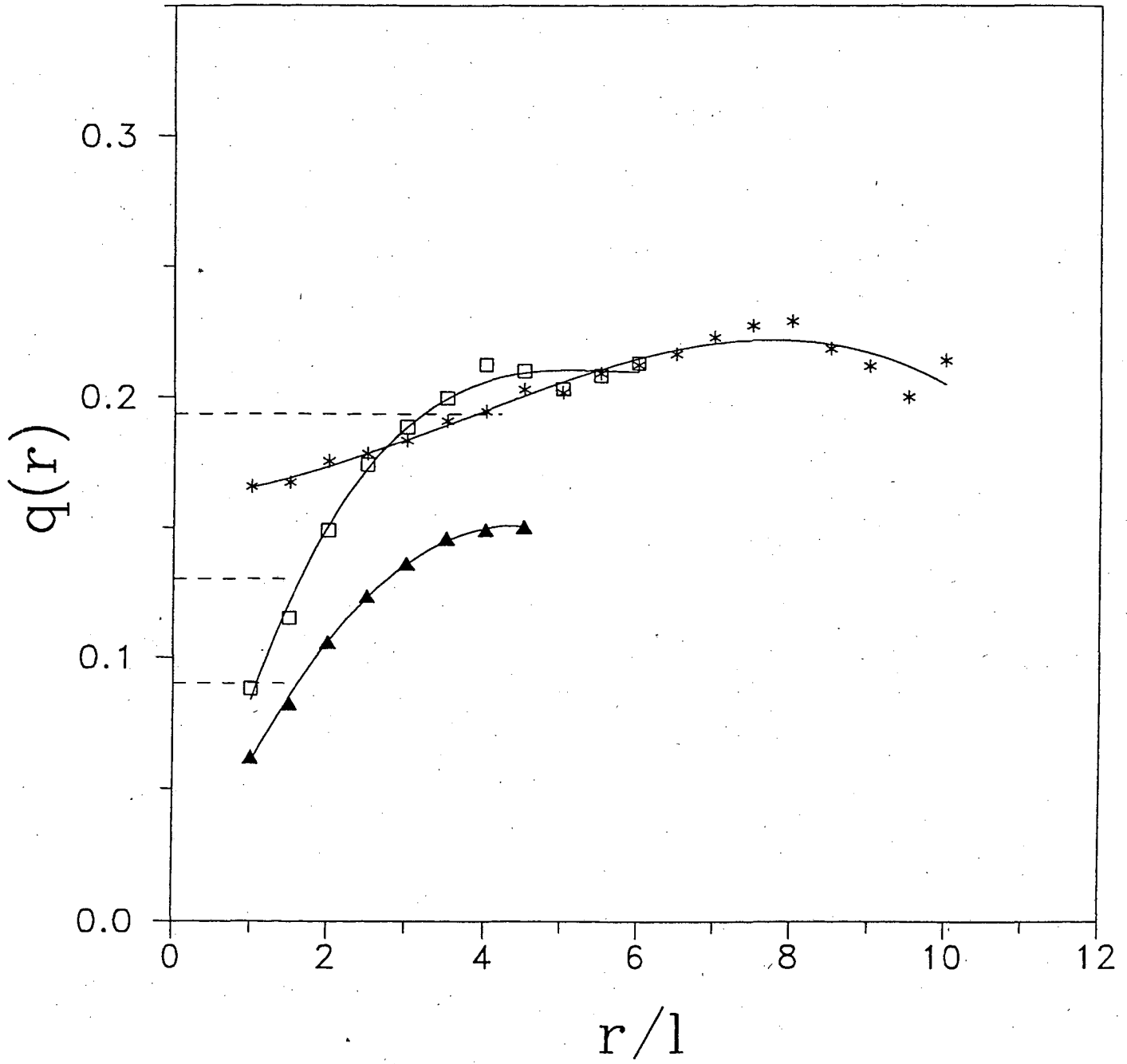24. A.R. Khokhlov, J. Phys. A, 13, 979 (1980).
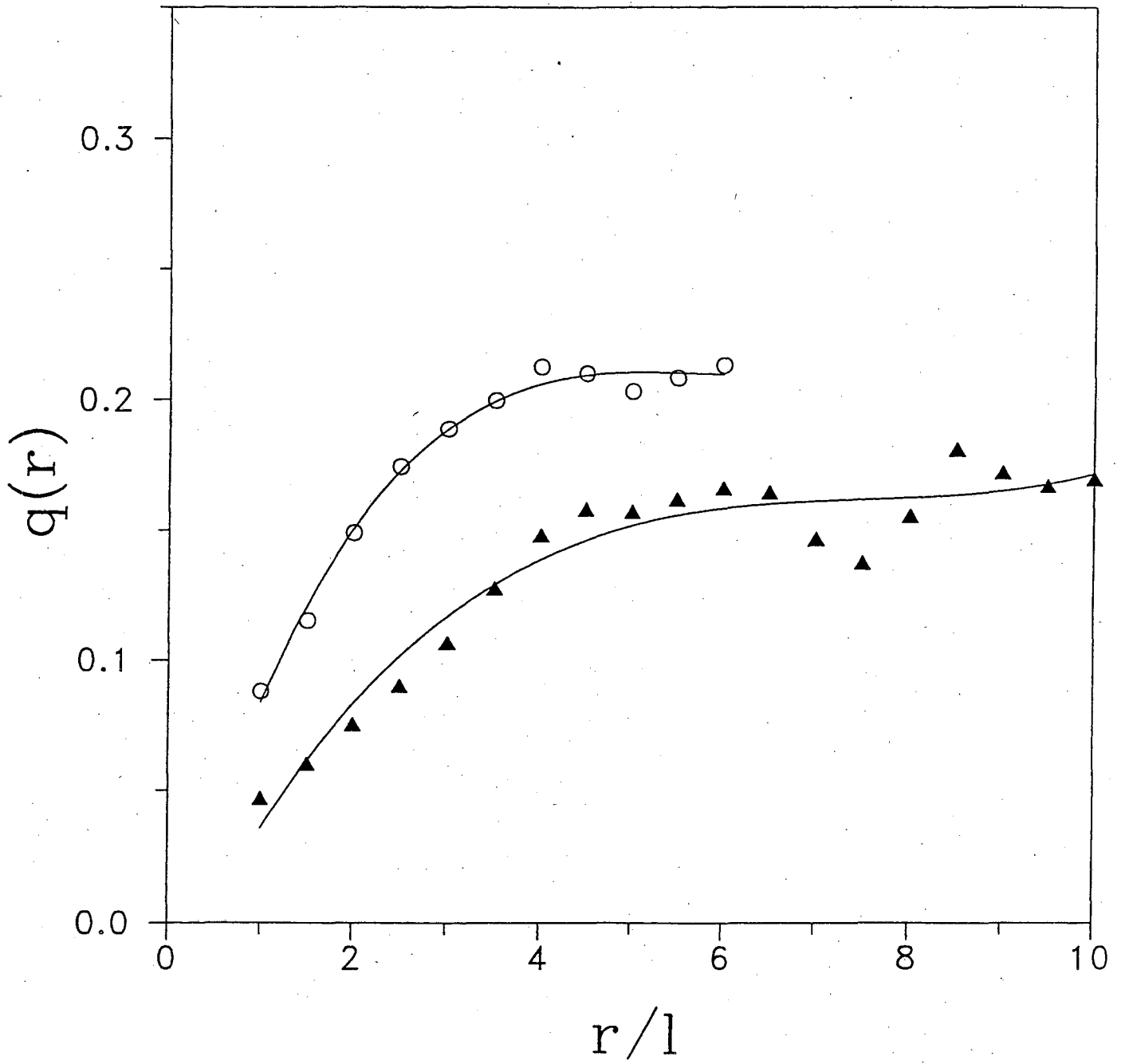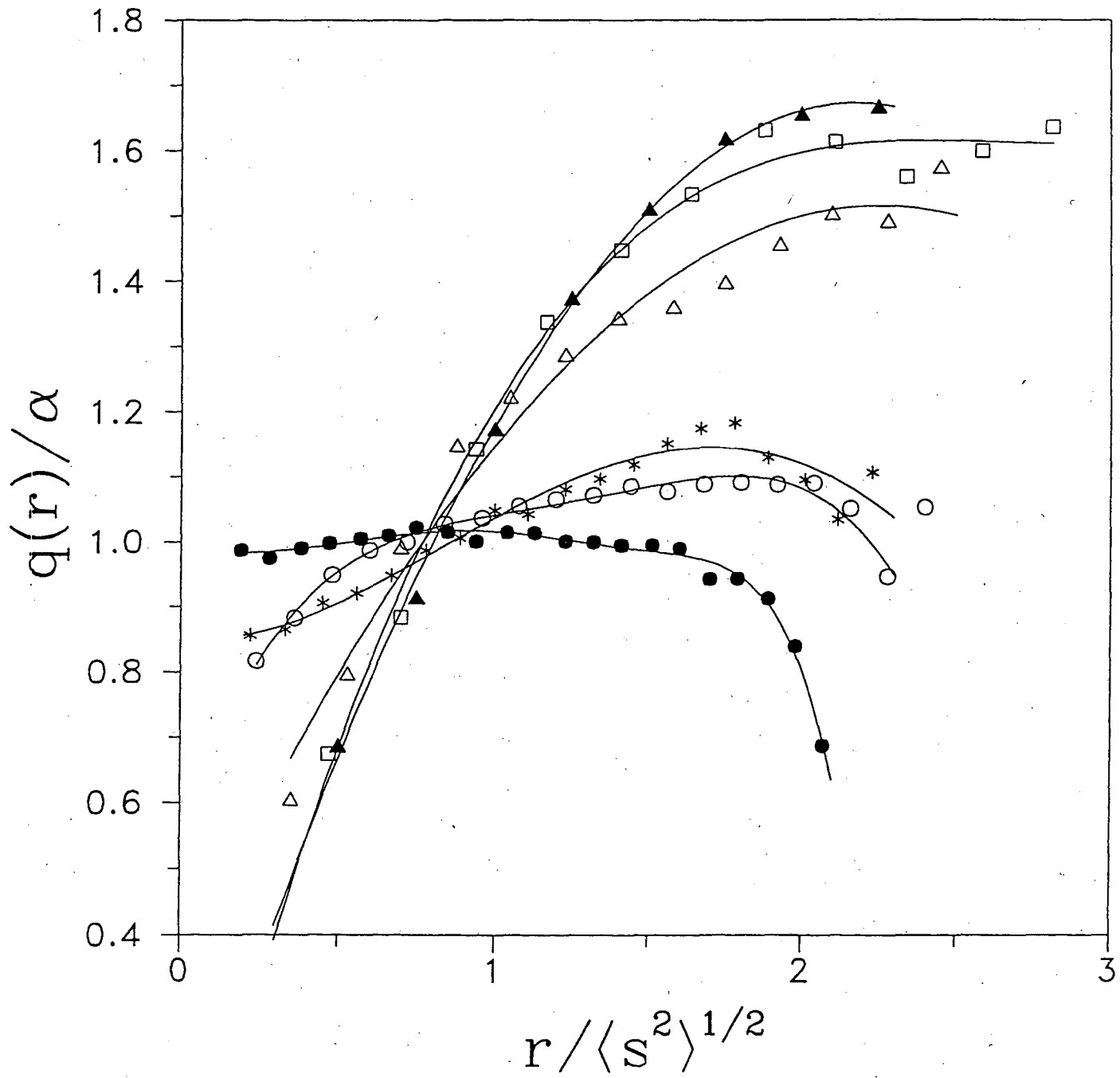
FIGURE 1

FIGURE 2

FIGURE 3

FIGURE 4

LAWRENCE BERKELEY LABORATORY
UNIVERSITY OF CALIFORNIA
TECHNICAL INFORMATION DEPARTMENT
BERKELEY, CALIFORNIA 94720